International Journal of Environmental Sciences
ISSN: 2229-7359
Vol. 11 No. 23s, 2025
https://theaspd.com/index.php

Novel Use of Deep Learning for Adaptive Weighted Loss in the Segmentation of X-ray Images for Detecting Wrist Fractures

Teuku Radillah[1], Sarjon Defit[2], Gunadi Widi Nurcahyo[3]
[1]Mitra Gama Institute of Technology
[2]University of Putra Indonesia YPTK Padang
[3]University of Putra Indonesia YPTK Padang
[1]t.radillah@gmail.com, [2]sarjon_defit@upiyptk.ac.id, [3]gunadiwidi@yahoo.co.id

Abstract– *Image transmission technology has made significant contributions to various fields, especially medical imaging, which employs X-ray imaging to detect abnormalities in the human body, such as cracks and fractures. The image segmentation method is a computational method that can divide digital images into several segments with similar visual characteristics. This research proposes a novel image segmentation method for wrist fractures, utilising an adaptive weighted-loss approach. The objective is to enhance the precision of identifying wrist fractures on X-ray images, with the target being an accuracy of 71%, a precision of 78%, a recall of 85%, and an F1-score of 81%. This study addresses a significant gap in the literature by proposing an effective method for identifying wrist fractures, a task for which there has been a dearth of effective methods. The adaptive weighted-loss method with linear weights proposed in this study is expected to overcome the challenges posed by overfitting and correct class imbalance, thereby ensuring that the model is not overly dependent on a single loss function. This approach is anticipated to enhance the model's generalisation capabilities on test data.*
Index Terms– *Dice Loss and BCE Loss method, Adaptive Weighted Loss, Wrist Fractures.*

I. INTRODUCTION

Image segmentation is a fundamental component of the image processing stage, which involves the separation of multiple regions or segments based on specific characteristics. The objective of this process is to identify and differentiate particular objects, components, or regions within the image that exhibit similarities in properties such as colour, intensity, texture, or shape. [1]. The image segmentation method is a computational technique that is capable of dividing digital images into multiple segments that exhibit similar visual characteristics. [2].

A number of segmentation methodologies are frequently employed, including texture-based segmentation, contouring, pixel selection and mathematical morphology. [3]. In the context of X-ray-based image segmentation, the prevailing algorithms employed are Dice Loss and BCE Loss. The Dice Loss function has been specifically optimised for segmentation tasks, as it directly measures the similarity between predictions and labels based on the Dice Coefficient.[4]. This method has been demonstrated to be effective in enhancing performance at boundaries between

objects and background, a capability that is frequently essential in medical segmentation, particularly in the detection of wrist fractures. The BCE Loss method quantifies the discrepancy between the predicted pixel probability and the correct binary label [5]. This process has been shown to be highly effective in addressing issues of class imbalance that frequently emerge in the context of X-ray images, where the area of an object (e.g., a fracture) may be significantly smaller in comparison to the background.The capture of internal images of the human body is achieved through the utilisation of a range of imaging techniques. These encompass X-ray-basedmethods, such as radiology, computed tomography, and mammography, alongside molecular imaging techniques and other modalities, including magnetic resonance imaging and ultrasonography. X-rays, a type of electromagnetic radiation with a short wavelength, possess the ability to penetrate certain solid materials, including human tissue.[6]. X-ray technology is utilised within the medical and scientific domains for the purpose of producing internal images of objects or the human body. [7]. X-ray images are also referred to as radiographic images or X-ray images. [8]. The process of taking an X-ray image involves the application of X-rays through a solid object, such as a human body or the object to be examined. The X-rays that pass through the object in question will create an image on a sensitive film or digital sensor, which is then arranged in a radiographic image. Subsequent to this, these images can be interpreted by a doctor or radiologist to aid in diagnosis and treatment planning. [9].

International Journal of Environmental Sciences
ISSN: 2229-7359
Vol. 11 No. 23s, 2025
https://theaspd.com/index.php

This research study proposes an innovative approach to analysing wrist fractures by developing an adaptive weighted loss image segmentation method, namely linear weighting. To evaluate the efficacy of the dice loss and BCE loss methods in conjunction with linear weighting, the U-Net model was employed, with an image pixel size of 256 X 256. As previously mentioned, wrist fractures are still challenging to detect using segmentation algorithms on X-ray images or CT scans. This research proposes an adaptive weighted loss image segmentation method, namely linear weighting, to address this issue. The effectiveness of this method is evaluated through experimentation with the dice loss and BCE loss methods with linear weighting. For this purpose, the U-Net model is applied, employing images resized to a pixel dimension of 256 x 256. The outcomes of this research enhance the existing knowledge base regarding wrist fracture detection via image segmentation techniques.[10]. The objective of this research is to develop an X-ray image segmentation method using adaptive weighted loss, namely linear weighting, to detect wrist fractures with a higher level of accuracy, and to determine the object of the wrist fracture with clearer image segmentation results.

.

II. RESEARCH METHOD

As illustrated in the block diagram below, the development of the adaptive weighted loss method for dice loss and BCE loss in the process of identifying cracks and fractures in wrist bones is evident.:

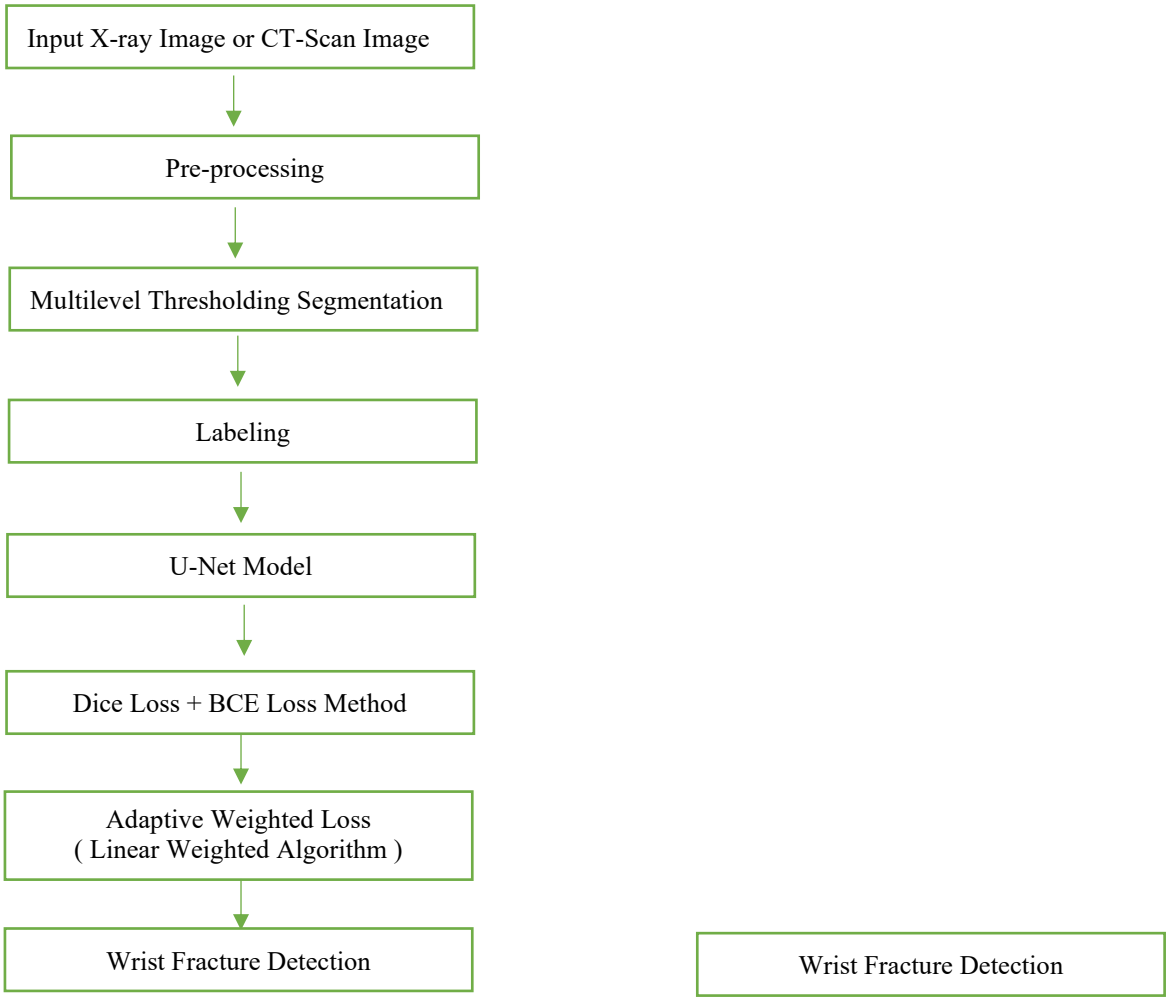

fig 1. Wrist fracture detection steps

The detection of wrist fractures is achieved through the analysis of X-ray and CT-Scan images, which are composed of photographs depicting various types of wrist bone fractures. Subsequent processing of these images involves a series of operations, including cropping, normalization, resizing, contrast stretching, and augmentation. The application of filters and histogram equalisation is also a key component of the analysis..

The processing results are then subjected to segmentation using the multilevel thresholding method, with

the aim of dividing the crack area into various levels. [11]. The subsequent stage of the process involved the annotation of each fracture in the wrist bone. Following the completion of the multilevel thresholding segmentation, the X-ray images that exhibited cracks were subjected to bounding, with the objective of their subsequent classification into training data and test data. The dice loss and BCE loss methods are then combined using adaptive weighted loss, namely linear weighting, to accelerate model convergence without compromising segmentation quality.

A. Wrist Fracture

A wrist fracture is defined as a fracture of the bones in the wrist. [12]. The wrist is composed of eight small bones known as the carpal bones, in addition to the distal ends of the two long bones in the forearm, namely the radius and ulna[13]. The collective arrangement of these bones facilitates the formation of the wrist joint. Distal radius fractures are a prevalent type of fracture, often occurring in the distal radius bone, which is located in close proximity to the distal end of the wrist. [14], The next anatomical structure to be examined is the scapoid, which is a carpal bone that frequently fractures when an individual falls with their arms outstretched. Due to its location and the fact that it is not visible on initial X-rays, fractures in this bone are difficult to diagnose.[15]. A further fracture has been identified in the distal ulna. Although not common, a fracture to the distal end of the ulna can occur, often in conjunction with a fracture to the distal radius. A fracture to the lunate is frequently associated with dislocation or other complex injuries..

The manifestation of symptoms in cases of wrist fracture may vary depending on the severity of the fracture and its anatomical location. [16], The common symptoms of a wrist fracture include pain, swelling and increased sensitivity, broken bones, limited movement, broken skin or open skin, and a tingling or numb sensation.

(a) Original Image (b) s

fig 2. Wrist Fracture X-ray Photo Segmentation

A. Datasets

This study uses a sample of 160 x-ray and CT-Scan wrist fracture data consisting of images of cracks and fractures in the wrist obtained from the Dumai Regional General Hospital (RSUD) and from www.kaggale.com. The dataset consists of 120 training data and 40 test data of x-ray and CT-Scan photos..

B. Dice Loss

Dice Loss is a loss function used primarily in image segmentation tasks, especially for medical segmentation. [17]. Dice Loss is derived from the Dice Coefficient, a statistical metric developed to quantify the similarity between two datasets. It is frequently utilised to assess the correspondence between a model's predictions and the actual labels, thus providing a reliable metric for evaluating segmentation performance.. [18]. The Dice Loss formula [19] is as follows :

$$\text{Dice Loss} = 1 - \frac{2 \cdot TP}{2 \cdot TP + FP + FN} \quad (1)$$

Where :

TP = (True Positives) number of truly positive and predicted positive pixels.

FP = (False Positives the number of pixels that are negative but predicted to be positive.

The main purpose of applying Dice Loss is to improve model performance on segmentation tasks, especially in the context of medical image processing or other tasks where there is significant class imbalance. Dice Loss directly measures the similarity between the model prediction and the correct label. For medical image processing such as X-Ray image segmentation, dice loss provides a more effective way to measure and optimise model performance compared to other loss methods.

C. BCE Loss

Binary Cross-entropy (BCE) is a loss function often used in binary classification tasks, including object detection and image segmentation in deep learning. [20]. The BCE Loss formula is as follows:

$$\text{BCE Loss1} = -\frac{1}{N} \sum_{i-1}^{N} (y_i . \log(p_i) + (1-y_i). \log(1-p_i)) \quad (2)$$

Where :

y_i = original label (0 or 1)

p_i = model prediction probability (value between 0 and 1)

N = number of pixels

The purpose of applying Binary Cross-Entropy (BCE) Loss is to measure how well a binary classification model predicts the correct output. BCE Loss provides a quantitative evaluation of how far the model's prediction is from the true target value, and is particularly useful for binary classification tasks, where the model must choose between two classes (e.g., 0 and 1).[21]. This function is well suited for measuring the probability of prediction compared to the correct binary label, in addition BCE Loss can be used with adjustments to handle class imbalance, such as by giving additional weight to the minority class, so that the model does not just learn to predict the majority class well.[22].

D. Adaptive Weighted Loss

Adaptive weighted loss is a technique used in training learning models, especially in image segmentation to weight the contribution of each loss function component. [23]. In this research, the weight given uses a linear weighting algorithm in the Dice and BCE Loss methods. The purpose of applying Adaptive weighted loss is to improve model performance by focusing attention on certain areas or parts of the data that are considered more important, or to overcome the imbalance between classes in the image. The Linear Weighted Algorithm formula applied to Adaptive weighted loss is as follows:

$$\alpha(t) = \alpha_{start} + (\alpha_{end} - \alpha_{start}) \cdot \frac{t}{T}$$

$$\beta(t) = \beta_{start} + (\beta_{end} - \beta_{start}) \cdot \frac{T-t}{T} \quad (3)$$

Where :

$\alpha(t)$ and $\beta(t)$ are time functions that adjust the weights as the training progresses.

t = current epoch or iteration

T = total number of epochs or training iterations

α_{start}., α, βstart, β_{end} are parameters that determine the initial and final values of the adaptive weights.

$(y_i . \log(p_i) + (1-y_i). \log(1-p_i))$

E. Evaluation Criteria

To evaluate the criteria in testing the development of segmentation algorithms on x-ray images in this study using accuracy, precision recall and F1 score metrics. [24]. The accuracy metric is used for the total correct predictions out of all available predictions[25], while recall is used for the proportion of wrist fracture cases identified, and precision metrics are used to measure the proportion of predicted fractures from the total x-rays or CT-Scans that have a fracture of the wrist bone..

$$\text{Accuracy} = \frac{TP + TN}{FP + TP + FN + TN} \quad (4)$$

$$\text{Recall} = \frac{TP}{TP + FN} \quad (5)$$

$$\text{Precision} = \frac{TP}{TP + FP} \quad (6)$$

$$\text{F1\_Score} = 2.\frac{\text{Precision} \cdot \text{Recall}}{\text{Precision} + \text{Recall}} \quad (7)$$

III. RESULT AND DISCUSSION

The results of the development of a segmentation algorithm on x-ray images to detect wrist bone cracks use the Matlab 2024a application in the pre-processing stage, while in the process of segmentation and detection of wrist bone cracks using Python 3.11.1 For Windows using the U-Net model..

A. Pre-procesing

Pre-processing in image segmentation is a stage performed to prepare the image before applying segmentation techniques. Pre-processing is done to improve image quality, reduce noise, and ensure that important features in the image can be recognised more easily by the segmentation algorithm. The following are some common techniques used in image preprocessing for segmentation in research consisting of cropping, normalisation, resizing, contrast stretching, augmentation, filterimg, histogram equalisation, and multileve thresholding segmentation. Furthermore, the image is labelled with a bounding box on the bone area that has fractures such as cracks and fractures. The labelling results will be stored in the training data (train_mask) and test data (test_mask) folders.

(a) Original Image (b) Cropping

fig 3. Original image of Wrist Fracture x-ray photo after cropping

B. Dice and BCE Loss Labeling and Segmentation Result

The result of labelling using bounding box on the area of the wrist bone that has a fracture or bone fracture.

TABLE I. LABELING AND SEGMENTATION RESULT

No	Labeling	Segmentation Result
1		
2	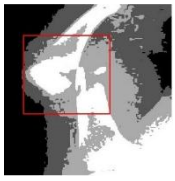	
3	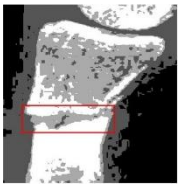	

4		
5	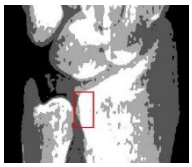	
...	.....	.....
...	.....	.....
39		
40	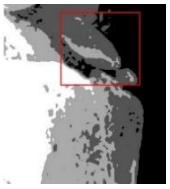	

The segmentation results of the Dice and BCE Loss methods before development show the overall metric evaluation results, namely Accuracy: 0.7076, Precision: 0.8092, Recall: 0.8063 and F1-Score: 0.8077. Apart from the information contained in Table I, The outcomes of the training and validation processes are further illustrated through the graphical representation of loss trends observed at each epoch, as depicted in Figure 4. This visualization provides a clearer understanding of the model's performance progression over the training phases.

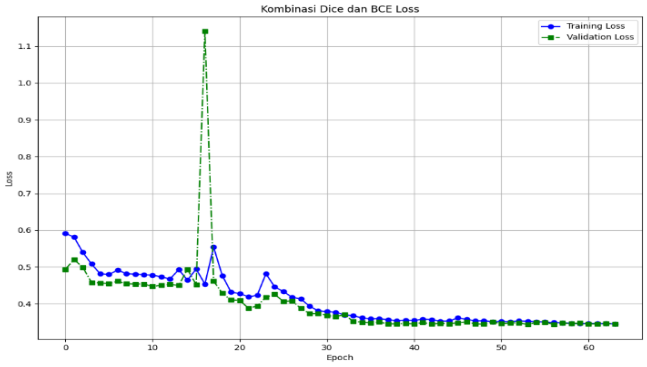

fig 4. Grafik Kombinasi Metode Dice dan BCE Loss

C. Adaptive Weighted Loss Development Results

The results of developing the Adaptive Weighted Loss method by applying the Linear Weighted Algorithm formula to the U-Net model in the callback training process, where in the training process the model can learn each image image at each epoch with dynamic weighting so that the accuracy and stability of the model in detecting fractures can be improved, especially in overcoming class imbalance. The evaluation results of the Adaptive Weighted Loss metrics for wrist fracture detection are presented in Table 2.

TABLE II. WRIST FRACTURE DETECTION RESULT

No	Fracture Detection Result	Accuracy	Precision	Recall	F1 Score	Description
1		0.7287	0.8285	0.8203	0.8244	Data Uji 1
2		0.7621	0.9014	0.8100	0.8532	Data Uji 2
3		0.7224	0.8228	0.8197	0.8212	Data Uji 3
4		0.6765	0.7884	0.7989	0.7936	Data Uji 4

No	Fracture Detection Result	Accuracy	Precision	Recall	F1 Score	Description
5		0.7734	0.8001	0.8625	0.8301	Data Uji 5
6		0.6735	0.7818	0.8048	0.7931	Data Uji 6
...	.....	.....	.....	.....	.....	.....
...	.....	.....	.....	.....	.....	.....
39		0.7064	0.8339	0.7776	0.8048	Data Uji 39
40		0.7609	0.8047	0.8282	0.8163	Data Uji 40

The segmentation results of the Dice and BCE Loss methods after development by displaying the overall metric evaluation results, namely Accuracy: 0.7134, Precision: 0.7873, Recall: 0.8543 and F1-Score: 0.8184. Apart from the information contained in Table 2, the results of training and validation can also be seen in the graphical display of loss at each epoch in Figure 5.

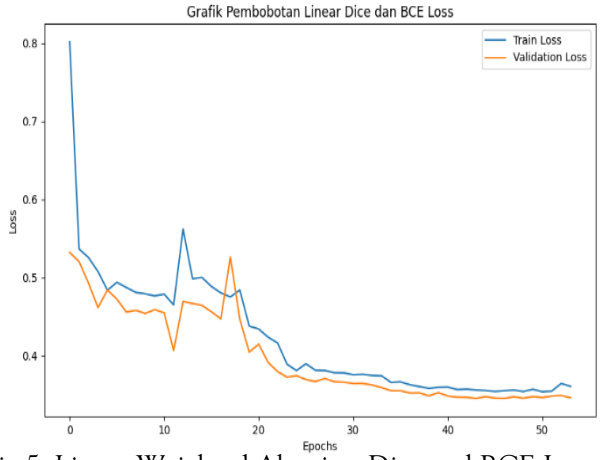

fig 5. Linear Weighted Algoritm Dice and BCE Loss

CONCLUSION

In this study, we have successfully developed and implemented an X-ray image segmentation algorithm using adaptive weighted loss method by applying linear weighted algorithm to detect wrist fracture with higher accuracy of 71%, precision of 78%, recall of 85% and F1-score of 81%. Experimental results show that the proposed approach is able to improve accuracy and efficiency in medical image segmentation compared to the Dice and BCE loss methods without using adaptive weighting. Use of linear weighted algorithm The application of linear weights to the combination of Dice Loss and BCE Loss in wrist fracture image segmentation can result in a more balanced and optimised performance. Dice Loss helps in measuring area similarity to detect small fractures, while BCE Loss focuses on probability classification of each pixel. By adjusting the linear weights, the accuracy and stability of the model in detecting fractures can be improved, especially in overcoming the class imbalance often found in medical images.

The performance of the algorithm was assessed using metrics such as accuracy, precision, recall and F1 score, all of which showed significant improvements. The algorithm was also tested on a dataset of wrist X-ray images with varying lighting conditions and different levels of cracks, and the results showed consistency in detecting cracks in the wrist bones.

ACKNOWLEDGEMENT

Our gratitude goes to the entire academic community, radiology specialists and orthopaedic specialists of Dumai Regional General Hospital, as well as to the promoters and co-promoters for providing advice and assisting in the completion of this study.

REFERENCES

[1]B. Abid, B. M. Khan, and R. A. Memon, “Seismic Facies Segmentation Using Ensemble of Convolutional Neural Networks,” Wirel. Commun. Mob. Comput., vol. 2022, 2022, doi: 10.1155/2022/7762543.

[2]R. Joshi, “Segmentation of Teeth in Panoramic X-ray Image Using U-net Algorithm,” 2024 3rd Int. Conf. Artif. Intell. Internet Things, AIIoT 2024, no. AIIoT, pp. 1–6, 2024, doi: 10.1109/AIIoT58432.2024.10574786.

[3]J. Zhang, Y. Zheng, and Y. Shi, “A Soft Label Method for Medical Image Segmentation with Multirater Annotations,” Comput. Intell. Neurosci., vol. 2023, no. 1, 2023, doi: 10.1155/2023/1883597.

[4]R. P. De Lima, B. Vahedi, and M. Karimzadeh, “Comparison of Cross-Entropy, Dice, and Focal Loss for Sea Ice Type Segmentation,” Int. Geosci. Remote Sens. Symp., vol. 2023-July, no. 2026962, pp. 145–148, 2023, doi: 10.1109/IGARSS52108.2023.10282060.

[5]J. Sun, Y. Li, X. Wu, C. Tang, S. Wang, and Y. Zhang, “HAD-Net: An attention U-based network with hyper-scale shifted aggregating and max-diagonal sampling for medical image segmentation,” Comput. Vis. Image Underst., vol. 249, no. September, p. 104151, 2024, doi: 10.1016/j.cviu.2024.104151.

[6]T. Anwar and S. Zakir, “Comparison of Loss functions and Optimizers for Multi-class X-ray Bone Segmentation,” 2nd IEEE Int. Conf. Artif. Intell. ICAI 2022, no. March 2021, pp. 33–37, 2022, doi: 10.1109/ICAI55435.2022.9773572.

[7]K. Jung, T. Duc Nguyen, D. T. Le, J. Bum, S. S. Woo, and H. Choo, “Hand Bone X-rays Segmentation and Congregation for Age Assessment using Deep Learning,” Int. Conf. Inf. Netw., vol. 2023-Janua, pp. 565–568, 2023, doi: 10.1109/ICOIN56518.2023.10048972.

[8]S. K. Jadwaa, “X-Ray Lung Image Classification Using a Canny Edge Detector,” J. Electr. Comput. Eng., vol. 2022, 2022, doi: 10.1155/2022/3081584.

[9]C. Yang, J. Ye, Y. Wang, and C. Song, “X-Ray Breast Images Denoising Method Based on the Convolutional Autoencoder,” Math. Probl. Eng., vol. 2022, 2022, doi: 10.1155/2022/2362851.

[10] D. Joshi, T. P. Singh, and A. K. Joshi, “Deep learning-based localization and segmentation of wrist fractures on X-ray radiographs,” Neural Comput. Appl., vol. 34, no. 21, pp. 19061–19077, 2022, doi: 10.1007/s00521-022-07510-z.

[11] A. Kumar, A. Kumar, and A. Vishwakarma, “Multilevel Thresholding of Grayscale Complex Crop Images using Minimum Cross Entropy,” Proc. 10th Int. Conf. Signal Process. Integr. Networks, SPIN 2023, pp. 806–810, 2023, doi:

10.1109/SPIN57001.2023.10117235.
[12] T. Anwar and H. Anwar, "LSNet: a novel CNN architecture to identify wrist fracture from a small X-ray dataset," Int. J. Inf. Technol., vol. 15, no. 5, pp. 2469–2477, 2023, doi: 10.1007/s41870-023-01311-w.
[13] K. Rachunek-Medved et al., "Do perilunate dislocations and fracture-dislocations result in different radiological outcomes following wrist alignment reconstruction? A single-center retrospective study including 51 patients with perilunate injuries," Arch. Orthop. Trauma Surg., vol. 145, no. 1, pp. 1–15, 2025, doi: 10.1007/s00402-024-05744-1.
[14] S. C. Medaramatla, C. V. Samhitha, S. D. Pande, and S. R. Vinta, "Detection of Hand Bone Fractures in X-Ray Images Using Hybrid YOLO NAS," IEEE Access, vol. 12, no. February, pp. 57661–57673, 2024, doi: 10.1109/ACCESS.2024.3379760.
[15] R. Kapse, S. Daware, R. Bawane, T. Cholkar, and D. Bambawale, "Image Processing for Detecting Bone Fractures," 2023 4th Int. Conf. Electron. Sustain. Commun. Syst. ICESC 2023 - Proc., pp. 1297–1302, 2023, doi: 10.1109/ICESC57686.2023.10193303.
[16] S. Mohanty and M. R. Senapati, "Fracture detection from X-ray images using different Machine Learning Techniques," 2023 1st Int. Conf. Circuits, Power, Intell. Syst. CCPIS 2023, pp. 1–6, 2023, doi: 10.1109/CCPIS59145.2023.10291652.
[17] F. Piri, N. Karimi, and S. Samavi, "Enhanced Segmentation in Abdominal CT Images: Leveraging Hybrid CNN-Transformer Architectures and Compound Loss Function," 2024 IEEE 5th World AI IoT Congr. AIIoT 2024, pp. 363–369, 2024, doi: 10.1109/AIIoT61789.2024.10579036.
[18] Z. Zhou, L. Cai, P. Yin, X. Qian, Y. Dai, and Z. Zhou, "Narrow-band loss - A novel loss function focused on target boundary," Proc. Annu. Int. Conf. IEEE Eng. Med. Biol. Soc. EMBS, pp. 1–4, 2023, doi: 10.1109/EMBC40787.2023.10340038.
[19] A. Alhudhaif, H. Ocal, N. Barisci, İ. Atacak, M. Nour, and K. Polat, "A Novel Approach to Skin Lesion Segmentation: Multipath Fusion Model with Fusion Loss," Comput. Math. Methods Med., vol. 2022, 2022, doi: 10.1155/2022/2157322.
[20] S. Koles, S. Karakas, A. P. Ndigande, and S. Ozer, "Using Different Loss Functions with YOLACT++ for Real-Time Instance Segmentation," 2023 46th Int. Conf. Telecommun. Signal Process. TSP 2023, pp. 264–267, 2023, doi: 10.1109/TSP59544.2023.10197832.
[21] M. Daraee, E. Saeedzadeh, P. Ghaffarian, and H. Arabi, "A Novel Context Loss Function Defined on the Feature Maps: Evaluation for Lesion Segmentation from PET Images versus Conventional Loss Functions," 2022 IEEE NSS/MIC RTSD - IEEE Nucl. Sci. Symp. Med. Imaging Conf. Room Temp. Semicond. Detect. Conf., 2022, doi: 10.1109/NSS/MIC44845.2022.10399025.
[22] T. H. Nguyen et al., "Systematic Evaluation of Loss Functions for Ovarian Tumors Segmentation from Ultrasound Images," 2023 1st Int. Conf. Heal. Sci. Technol. ICHST 2023, 2023, doi: 10.1109/ICHST59286.2023.10565336.
[23] J. Sun and D. Li, "A cloud-oriented siamese network object tracking algorithm with attention network and adaptive loss function," J. Cloud Comput., vol. 12, no. 1, 2023, doi: 10.1186/s13677-023-00431-9.
[24] A. Khanal, R. Rizk, and K. C. Santosh, "Ensemble Deep Convolutional Neural Network to Identify Fractured Limbs using CT Scans," Proc. - 2023 IEEE Conf. Artif. Intell. CAI 2023, pp. 156–157, 2023, doi: 10.1109/CAI54212.2023.00075.
[25] R. Velastegui, M. Tatarchenko, S. Karaoglu, and T. Gevers, "Image semantic segmentation of indoor scenes: A survey," Comput. Vis. Image Underst., vol. 248, no. July, p. 104102, 2024, doi: 10.1016/j.cviu.2024.104102.